

Atomic charge densities generated using an iterative stockholder procedure

Timothy C. Lillestolen and Richard J. Wheatley^{a)}

School of Chemistry, The University of Nottingham, Nottingham NG7 2RD, United Kingdom

(Received 15 May 2009; accepted 16 September 2009; published online 8 October 2009)

A simple computational technique is introduced for generating atomic electron densities using an iterated stockholder procedure. It is proven that the procedure is always convergent and leads to unique atomic densities. The resulting atomic densities are shown to have chemically intuitive and reasonable charges, and the method is used to analyze the hydrogen bonding in the minimum energy configuration of the water dimer and charge transfer in the borazane molecule. © 2009 American Institute of Physics. [doi:10.1063/1.3243863]

I. INTRODUCTION

One of the most widely held and successful concepts in chemistry is that a molecule is composed of its constituent atoms held together by chemical bonds and that molecular properties can be expressed as a sum of the individual atomic properties. The gap between rigorously defined *ab initio* molecular properties and the more conceptual chemical properties, which atoms and functional groups are known to possess based on scientific experience, are unsolved problems, as there is no unique way to partition the molecular electron density into a sum of its atomic components.

Methods for generating atomic electron densities can be broadly separated into two groups. The first involves basis set partitioning, of which the most common is the well-known Mulliken method.¹ These methods, however, commonly suffer from a marked dependence on basis set as well as yielding regions of negative atomic electron density. The second group is based on real space partitioning methods. The most well-known of these is Bader's Atoms in Molecules (AIM) approach.² This method generates atomic electron densities by using the topology of the molecular electron density to partition the molecule into atomic basins. The atomic electron density is then obtained by integrating over the atomic basin. The disadvantage of the method is that the atomic electron densities are discontinuous at the basin boundary, yielding highly nonspherical atoms. An alternative to the AIM approach is one introduced by Hirshfeld³ based on stockholder partitioning. The idea behind this approach is that the electron density at every point is distributed between all atoms based on a weighting function for each atom. This allows for atomic electron densities to overlap. In the original Hirshfeld approach, the weighting functions for each atom were based on the electron density of the isolated atoms in the gas phase, leading to atomic electron densities that are dependent on the choice of the isolated atom's electron configuration. This dependence is largely removed by the iterative Hirshfeld method (Hirshfeld-I) introduced by Bultinck *et al.*,⁴ however calculations of gas-phase electron densities are still required.

The present paper expands upon an iterative stockholder partitioning method,⁵ which allows for reasonably spherical overlapping atoms, requires no supplementary calculations, and is independent of the gas-phase atomic electron density. The theoretical basis for the iterative stockholder method is presented in Sec. II, methods for calculating iterative stockholder atoms (ISA) are presented in Sec. III, and results and conclusions are presented in Sec. IV. Atomic units are used in this paper. The physical constants $4\pi\epsilon_0$ (ϵ_0 =vacuum permittivity) and e (the elementary charge constant) both have the numerical value of one in atomic units. The atomic unit of length is the bohr, $a_0=5.291\,772\times 10^{-11}$ m, and the atomic unit of energy is the hartree, $E_h=4.359\,75\times 10^{-18}$ J.

II. THEORY

Atomic electron densities that are positive and exactly reproduce the molecular electron density may be generated via the stockholder method using spherically symmetric weighting functions $w_a(\mathbf{r})$ centered at the atomic nuclei a ,

$$\rho_a(\mathbf{r}) = \rho(\mathbf{r}) \frac{w_a(\mathbf{r})}{\sum_b w_b(\mathbf{r})}, \quad (1)$$

where $\rho(\mathbf{r})$ and $\rho_a(\mathbf{r})$ are the molecular and atomic electron densities at any point \mathbf{r} and the sum in the denominator is over all nuclei in the molecule. In the original stockholder method, atomic densities are calculated in the gas phase, spherically averaged, and then used as the weighting functions.

In the iterative stockholder procedure, no supplementary gas-phase calculations are required; a starting guess of $w_a(\mathbf{r})=1$ for all nuclei is used in Eq. (1) to generate the initial iteration of the atomic electron density $\rho_a(\mathbf{r})$. This density is then spherically averaged around the nucleus to generate the next iteration of weighting functions using

$$w_a(\mathbf{r}) = \langle \rho_a(\mathbf{r}) \rangle_a = \rho_a^0(\mathbf{r}), \quad (2)$$

where the angular brackets indicate a spherical average around nucleus a and the equivalent notation $\rho_a^0(\mathbf{r})$ is used

^{a)}Electronic mail: richard.wheatley@nottingham.ac.uk.

for brevity. The weighting functions generated using Eq. (2) are then used to generate new stockholder atoms via Eq. (1), which are in turn used to generate the next iteration of weighting functions. The process is repeated until both Eqs. (1) and (2) are solved simultaneously.

The simultaneous solution of Eqs. (1) and (2) is equivalent to minimizing the functional

$$F[\rho^0] = \int \rho^0 - \rho \ln \frac{\rho^0}{\rho} d\mathbf{r}, \quad (3)$$

with respect to the promolecule density ρ^0 and with the constraint that ρ^0 is the sum of positive spherical functions centered on the nuclei. The integral is over all space, and the \mathbf{r} dependence of the densities is not shown explicitly. The minimum possible value of $F[\rho^0]$ is equal to the number of electrons N_e and occurs when the promolecule density is equivalent to the molecular density, a case that will rarely happen in practice.

In order to show that the iterative procedure approaches the minimum of the functional $F[\rho^0]$, the promolecule density after iteration X can be written as

$$\rho^0(X) = \sum_a \rho_a^0(X). \quad (4)$$

Equations (1) and (2) are then applied to each atom a in turn to generate the next iteration, keeping all weighting functions involving nuclei other than a constant,

$$\rho_a^0(X+1) = \left\langle \frac{\rho_a^0(X)\rho}{\rho^0(X)} \right\rangle_a = \rho_a^0(X) \left\langle \frac{\rho}{\rho^0(X)} \right\rangle_a. \quad (5)$$

The condition for a minimum of $F[\rho^0]$ can be obtained by differentiating Eq. (3) with respect to spherically symmetric variations in ρ^0 about nucleus a , yielding

$$\left\langle \frac{\rho}{\rho^0} \right\rangle_{\text{shell},a} = 1. \quad (6)$$

If this is true following iteration X , i.e.,

$$\left\langle \frac{\rho}{\rho^0(X)} \right\rangle_{\text{shell},a} = 1, \quad (7)$$

further iteration via Eq. (5) leads to $\rho_a^0(X+1) = \rho_a^0(X)$. If Eq. (6) is not satisfied following iteration X , consider a single spherical shell centered on nucleus a for which

$$\left\langle \frac{\rho}{\rho^0(X)} \right\rangle_{\text{shell},a} = R < 1. \quad (8)$$

After the next iteration using Eq. (5),

$$\rho_a^0(X+1) = R\rho_a^0(X), \quad (9)$$

and this leads to the inequalities

$$R = \left\langle \frac{\rho}{\rho^0(X)} \right\rangle_{\text{shell},a} = \left\langle \frac{\rho}{\rho_a^0(X) + \sum_{b \neq a} \rho_b^0(X)} \right\rangle_{\text{shell},a} < \left\langle \frac{\rho}{R\rho_a^0(X) + \sum_{b \neq a} \rho_b^0(X)} \right\rangle_{\text{shell},a} = \left\langle \frac{\rho}{\rho^0(X+1)} \right\rangle_{\text{shell},a}. \quad (10)$$

and

$$\left\langle \frac{\rho}{\rho^0(X+1)} \right\rangle_{\text{shell},a} = \left\langle \frac{\rho}{R\rho_a^0(X) + \sum_{b \neq a} \rho_b^0(X)} \right\rangle_{\text{shell},a} < \left\langle \frac{\rho}{R\rho_a^0(X) + R\sum_{b \neq a} \rho_b^0(X)} \right\rangle_{\text{shell},a} = \frac{1}{R} \left\langle \frac{\rho}{\rho^0(X)} \right\rangle_{\text{shell},a} = 1. \quad (11)$$

The value of $\langle \rho/\rho^0 \rangle$ on nucleus a after iteration $X+1$ is between R and one and therefore is closer to the solution, Eq. (6); then it was after iteration X . A similar argument holds for $R > 1$ in Eq. (8), whereby iteration of $\rho^0(X)$ results in a value greater than one and less than R . It should be noted that for these arguments to hold, it is required that $\{\rho, \rho_a^0, \rho_b^0\} \geq 0$, which is always the case in the iterative scheme provided $\rho \geq 0$.

The functional in Eq. (3) can be shown to have a unique minimum by considering a small change to ρ^0 , i.e., $\rho^0 + \delta\rho^0$. Substituting into Eq. (3) yields

$$\begin{aligned} F[\rho^0 + \delta\rho^0] &= \int \rho^0 + \delta\rho^0 - \rho \ln \frac{\rho^0 + \delta\rho^0}{\rho} d\mathbf{r} = \int \rho^0 + \delta\rho^0 - \rho \ln \frac{\rho^0(1 + \delta\rho^0/\rho^0)}{\rho} d\mathbf{r} \\ &= \int \rho^0 + \delta\rho^0 - \rho \ln \frac{\rho^0}{\rho} - \rho \ln(1 + \delta\rho^0/\rho^0) d\mathbf{r} = F[\rho^0] + \int \delta\rho^0 - \rho \\ &\quad \times \left[\frac{\delta\rho^0}{\rho^0} - \frac{1}{2} \left(\frac{\delta\rho^0}{\rho^0} \right)^2 + \sum_{n=3}^{\infty} \frac{(-1)^{n+1}}{n} \left(\frac{\delta\rho^0}{\rho^0} \right)^n \right] d\mathbf{r} \\ &= F[\rho^0] + \int \left(1 - \frac{\rho}{\rho^0} \right) \delta\rho^0 + \frac{1}{2} \rho \left(\frac{\delta\rho^0}{\rho^0} \right)^2 + \sum_{n=3}^{\infty} \frac{(-1)^{n+1}}{n} \left(\frac{\delta\rho^0}{\rho^0} \right)^n d\mathbf{r}. \end{aligned} \quad (12)$$

The curvature of the functional is therefore always positive in every direction, so it has no maxima or saddle points and only one minimum. A similar proof of the uniqueness of the minimum is offered by Bultinck *et al.*⁶ The iterative procedure requires positive definiteness of the spherical atoms, a condition not required for minimization of the functional in Eq. (3). Alternative methods of minimizing $F[\rho^0]$ could consider regions of both positive and negative densities by replacing ρ with $|\rho|$ in Eq. (3) but not in Eq. (1).

Finally, it can be shown that when $F[\rho^0]$ is at the minimum, the integral of the spherical density over all space must equal the number of electrons N_e . Starting from Eq. (6),

$$\begin{aligned} \left\langle \frac{\rho \rho_a^0}{\rho^0} \right\rangle_a &= \rho_a^0, \\ \int \frac{\rho \rho_a^0}{\rho^0} d\mathbf{r} &= \int \rho_a^0 d\mathbf{r}, \\ \int \frac{\rho \sum_a \rho_a^0}{\rho^0} d\mathbf{r} &= \int \sum_a \rho_a^0 d\mathbf{r}, \\ \int \rho d\mathbf{r} &= \int \rho^0 d\mathbf{r} = N_e. \end{aligned} \quad (13)$$

In the iterative stockholder procedure, the condition $\int \rho^0 d\mathbf{r} = N_e$ is not only fulfilled at the minimum but also after each iteration.

III. METHODS

In order to calculate the spherically averaged densities in Eq. (2) and the functional in Eq. (3) and to evaluate atomic charges and multipoles, a suitable method of integration over the molecular volume must be chosen. Much work has been done on this problem with respect to the integration of the exchange-correlation functional in density functional theory (DFT) over molecular volume.^{7,8} In DFT integration, the integral of an arbitrary function $F(\mathbf{r})$ is partitioned into atom-centered regions, and then a sum over all regions approximates the molecular integral,

$$\int F(\mathbf{r}) d\mathbf{r} = \sum_{\text{atoms}, r, \Omega} w_{\text{Becke}} w_r w_{\Omega} F(r, \Omega), \quad (14)$$

where the sum is over atoms, radial grid points, and angular grid points and $F(r, \Omega)$ is the function evaluated at a given grid point. The Becke partitioning scheme⁷ is used to generate the Becke weights w_{Becke} , the method of Mura and Knowles (Log3) to generate the radial grid points and weights, w_r ,⁸ and the angular grid points of Lebedev and Laikov⁹ are used with weights $w_{\Omega} = 4\pi/n_{\Omega}$, where n_{Ω} is the number of points in the angular shell. The atomic charges of the iterated stockholder atoms are then obtained from

$$q_a = Z_a - \sum_{\text{atoms}, r, \Omega} w_{\text{Becke}} w_r w_{\Omega} \rho_a(r, \Omega) \quad (15)$$

where Z_a is the nuclear charge and $\rho_a(r, \Omega)$ is the iterated stockholder density obtained using the methods of Sec. II.

In order to generate the spherical average in Eq. (2), it is necessary to average each radial shell over its constituent angular points. Since all w_{Ω} are the same within a radial shell,

$$\rho_a^0(r_i) = \frac{1}{n_{\Omega}} \sum_{\Omega} \rho_a(r_i, \Omega), \quad (16)$$

where $\rho_a^0(r_i)$ is the spherically averaged density of the i th radial shell. To calculate the next iteration of the atomic densities using Eq. (1), it is then necessary to obtain the spherical density of every atom a at every grid point not only those belonging to (i.e., in the integration grid of) atom a . Equation (16) enables $\rho_a^0(r_i)$ to be calculated for all radii r_i of radial shells of grid points for atom a but not in between those values. In order to obtain the spherical density of atom a on a grid point belonging to atom b , the distance r_a of the point to center a is calculated, and exponential interpolation of ρ_a^0 is used between the two radial shells of atom a bracketing r_a . Points outside the largest radial shell of atom a are assigned a value of $\rho_a^0 = 0$. This is not found to affect the results within the precision of the numerical integration. A single iteration of the iterated stockholder method starting from a set of weighting functions therefore consists of calculating atomic densities at every grid point using Eq. (1), spherically averaging these for each atom at grid points belonging to that atom using Eq. (16), and finally interpolating these to grid points belonging to all other atoms. The spherically averaged atomic densities are then used as weighting functions for the next iteration until self-consistency is achieved, which is defined for iteration X using

$$\delta = \sum_a \sum_i^{n_r} r_i^2 |\rho_a^0(i, X) - \rho_a^0(i, X-1)|, \quad (17)$$

where $\delta < 10^{-6}$ is taken to be converged.

In order to investigate the dependence of the ISAs on grid size, ISAs are calculated using different radial and angular grids. The ISAs are found to be less sensitive to the angular grid than to the radial grid, and a standard angular grid (grid 4)¹⁰ is found to be sufficient. Increasing the angular grid is not found to have an effect on ISA charges, dipoles, or quadrupoles, but if higher order multipoles are needed, it may be necessary to increase the number of angular points. Figure 1 shows the ISA charges of HCONH₂ calculated at the B3LYP (Ref. 11)/aug-cc-pVDZ (Ref. 12) level of theory using an increasing number of radial points with the same angular grid. The ISA charges are found to be converged to the nearest hundredth of an electron when 80 radial points are used for hydrogen and 85 for heavier elements.

IV. RESULTS AND CONCLUSIONS

In order to demonstrate the utility of the iterated stockholder procedure, the first molecule chosen for study is LiF. A well-known deficiency of the original Hirshfeld procedure is that the final charges obtained are highly dependent on the initial spherical atomic density; in the case of LiF, an initial guess of Li⁺-F⁻ yields different results for the final charges than an initial guess of Li-F or Li⁻-F⁺. This deficiency is

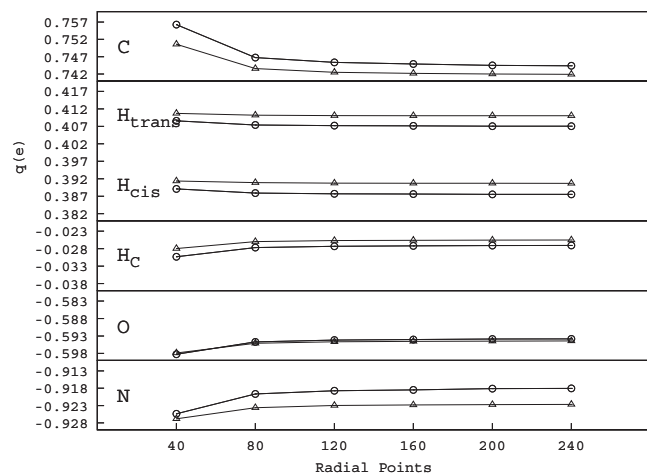


FIG. 1. Charges of iterated stockholder atoms calculated as a function of radial grid size. The x axis shows the number of hydrogen radial points; five more radial points are used for heavier elements.

overcome in the iterative Hirshfeld procedure of Bultinck *et al.*⁴ as well as the current method because they are independent of the initial guess. Using the B3LYP/aug-cc-pVTZ method with a bond length of $3.022 a_0$ and starting from initial weighting functions of $w_{\text{Li}}(\mathbf{r})=1$, $w_{\text{F}}(\mathbf{r})=1$, a final charge of $\pm 0.969 e$ is found for each atom. These charges are close to the values $\pm 1 e$ that would be expected for a bond with ionic character. Fitting the charges to the LiF dipole, $\mu_z=2.624 e a_0$, yields $\pm 0.868 e$ for the atoms. The difference between the dipole calculated using the ISA charges and the molecular dipole must arise due to atomic dipoles. In accord with physical intuition, the ISA method predicts that it is mainly the F atom that is polarized, having a dipole of $\mu_z=-0.321 e a_0$, whereas the ISA Li atom has $\mu_z=0.006 e a_0$.

The general applicability of the iterated stockholder procedure is further demonstrated by applying it to the case of ions. Table I shows ISA and Mulliken¹ charges for a variety of ions and the corresponding conjugate acids and bases calculated using the B3LYP/aug-cc-pVQZ method. The structure of each molecule is optimized using MOLPRO (Ref. 13) at the B3LYP/aug-cc-pVDZ level of theory using the highest point group available. The basis set dependence of the ISA charges is small; the average difference between values calculated with the aug-cc-pVDZ and aug-cc-pVQZ basis sets is $0.007 e$. The average difference between the aug-cc-pVTZ and aug-cc-pVQZ basis sets is even smaller, $0.001 e$, indicating that the results are effectively converged with respect to basis set at the aug-cc-pVTZ level. It is therefore the aug-cc-pVTZ basis that is used throughout this study. The Mulliken method gives reasonable charges for all of the molecules; however the basis set dependence is large with an average difference between the aug-cc-pVDZ and aug-cc-pVQZ basis sets of $0.303 e$. Although atomic charges are arbitrary quantities, the ISA results in Table I are generally in accord with chemical intuition, with more electronegative atoms generally having more negative charges, acidic hydrogens being positively charged, and chemically similar atoms having similar charges.

The water dimer provides a demonstration of the utility

TABLE I. B3LYP ISA and Mulliken charges calculated using the aug-cc-pVQZ basis set. Units of charge are e .

	Mulliken	ISA
ClO^-		
O	-0.875	-0.679
Cl	-0.125	-0.321
HOCl		
O	-0.520	-0.410
Cl	0.184	-0.002
H	0.336	0.413
CO_3^{2-}		
C	0.722	1.455
O	-0.907	-1.152
H_2CO_3		
C	1.103	1.038
O_c	-0.540	-0.690
O_H	-0.573	-0.627
H	0.320	0.453
NH_3		
N	-0.696	-1.021
H	0.232	0.340
NH_4^+		
N	-0.276	-0.725
H	0.104	0.431
OH^-		
O	-1.160	-1.291
H	0.160	0.291
H_2O		
O	-0.598	-0.834
H	0.299	0.417
H_3O^+		
O	-0.214	-0.723
H	0.405	0.574
CN^-		
C	-0.667	-0.500
N	-0.333	-0.500
HCN		
C	-0.111	0.070
N	-0.446	-0.304
H	0.557	0.234
NO_3^-		
N	0.796	1.180
O	-0.599	-0.727
HNO_3		
N	0.908	0.944
O_H	-0.436	-0.536
O_{cis}	-0.426	-0.460
O_{trans}	-0.383	-0.388
H	0.337	0.440
H_2CN^-		
C	-0.352	0.426
N	-0.855	-0.922
H	0.104	-0.252
H_3CN		
C	-0.588	0.134
N	-0.519	-0.587
H_{cis}	0.384	0.054
H_{trans}	0.452	0.086
H_N	0.271	0.312

of ISAs applied to hydrogen bonded systems. The second-order Møller-Plesset (MP2) electron density is used to calculate the ISAs using the aug-cc-pVTZ basis set. The OH bond length in water is fixed at $1.8361 a_0$, and the HOH bond angle at 104.69° ,¹⁴ with the oxygen atom located at the origin and the hydrogen atoms located at $(\pm x, 0, -z)$. For the

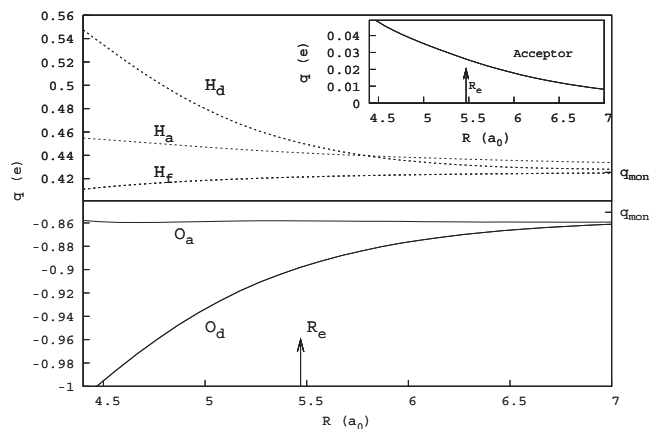


FIG. 2. Charges of iterated stockholder atoms in the water dimer. The subscript $a(d)$ refers to the hydrogen bond acceptor (donor), f refers to the free hydrogen on the proton donor, and q_{mon} is the charge of the atom in the isolated monomer. The overall charge transfer to the acceptor water monomer is shown in the inset.

$\text{H}_2\text{O}\cdots\text{H}_2\text{O}$ system, the minimum energy water dimer geometry as determined by van Duijneveldt-van de Rijdt *et al.*¹⁵ based on the calculations of Smith *et al.*¹⁶ is used. In order to investigate the effects of charge transfer and dipole polarization on the monomers, the distance R between the monomers is then varied between 4.4–7.0 a_0 . The Euler angles describing the dimer at the minimum are $(\alpha_1, \beta_1, \gamma_1) = (-180^\circ, 124.79^\circ, 0^\circ)$ and $(\alpha_2, \beta_2, \gamma_2) = (0^\circ, 134.15^\circ, -90^\circ)$, and monomer 2 is translated relative to monomer 1 by a distance R along the $+z$ direction. Figure 2 shows the ISA charge of each of the atoms along with the overall charge of the proton acceptor (i.e., the sum of its ISA charges). At the equilibrium bond length, an overall charge of +0.026 e is found for the proton acceptor. The amount of charge transferred is found to be exponential over a large range of bond lengths, with $\ln q(\text{acceptor}) \approx x + yR$. The ISA charges of the donor molecule show the largest changes, with the donor proton becoming more positive, while the donor oxygen becomes more negative when the hydrogen bond is formed. A reconstruction of the molecular dipole for each monomer using the monomer ISA charges shows good agreement, indicating that only changes in the atomic charges can be used to obtain qualitative trends in bonding processes. Polarization of the donor molecule is therefore shown in an ISA picture to consist mainly of electron transfer from H_d to O_d .

The borazane molecule H_3BNH_3 provides a further demonstration of the ISA method applied to charge transfer complexes. The MP2 electron density is used along with the aug-cc-pVTZ basis set to calculate the ISAs. The MP2 optimized C_{3v} eclipsed and staggered geometries of Jagielska *et al.*¹⁷ are used to examine the charge transfer. The staggered geometry conforms to the global energy minimum, while the eclipsed conformation is a saddle point. In the staggered complex the amount of ISA charge transferred corresponds to $-0.383 e$ ($-0.384 e$ for the eclipsed complex) transferred from the NH_3 monomer to the BH_3 monomer, as shown in Table II. The trends are similar for both complexes; a comparison of the individual ISA charges between the monomers and staggered complex shows that the majority of

TABLE II. MP2 ISA charges for the borazane charge transfer complex and monomers BH_3 and NH_3 calculated using the aug-cc-pVTZ basis set. Units of charge are e .

	B	H _B	N	H _N
Monomers	0.626	-0.209	-1.072	0.357
Eclipsed	0.392	-0.259	-0.588	0.324
Staggered	0.386	-0.256	-0.607	0.330

the charge is transferred between the boron and nitrogen, with smaller amounts being transferred to/from the hydrogens.

The radial behavior of the spherically averaged ISA atoms is fitted to a spherically symmetric function $\tilde{\rho}_a^0$ by minimizing the residual quantity

$$Z_a(\theta) = \int \int [\rho_a^0(\mathbf{r}_1) - \tilde{\rho}_a^0(\mathbf{r}_1)] \theta(r_{12}) \times [\rho_a^0(\mathbf{r}_2) - \tilde{\rho}_a^0(\mathbf{r}_2)] d\mathbf{r}_1 d\mathbf{r}_2, \quad (18)$$

where $\theta(r_{12})$ is the fitting criterion chosen to be $1/4\pi\epsilon_0 r_{12}$, which fits the electric field.¹⁸ The fit is constrained to reproduce the number of ISA electrons N_e . The fitting functions $\tilde{\rho}_a^0$ are chosen to be either a single exponential ($c_1 e^{-\zeta_1 r}$) in the case of hydrogen or a biexponential ($c_1 e^{-\zeta_1 r} + c_2 e^{-\zeta_2 r}$) for second row atoms. Results are shown in Table III for NO_3^- and CO_3^{2-} as well as their conjugate acids. The radial densities are calculated using the B3LYP/aug-cc-pVTZ method using the previously optimized aug-cc-pVDZ geometries. The values of $Z(\theta)$ obtained using the exponential fits are several orders of magnitude less than the Coulomb self-interaction energy (I) of the spherical densities, indicating that the exponential functions are a good fit to the spherical density. Results for the first-row atoms consistently show an “inner shell” with a large exponent that remains fairly constant between atoms of the same type and a “valence shell” with a

TABLE III. Best fits to the B3LYP spherical charge density using Eq. (18) with the aug-cc-pVTZ basis set. The coefficients c'_i ($i=1,2$) are related to c_i by $c'_i = 8\pi c_i / \zeta_i^3$ so that $N_e = c'_1 + c'_2$. The units of $Z(\theta)$ and I^a are E_h .

	c'_1	c'_2	ζ_1	ζ_2	$Z(\theta)$	I^a
NO_3^-						
N	1.59	4.23	15.3	2.6	0.02	43.78
O	1.68	7.05	17.1	2.4	0.01	80.33
HNO_3						
N	1.62	4.44	15.2	2.5	0.02	45.29
O _H	1.62	6.92	17.5	2.5	0.02	79.21
O _{cis}	1.63	6.83	17.4	2.5	0.02	78.32
O _{trans}	1.65	6.74	17.3	2.5	0.02	77.75
H	0.56	...	2.8	...	0.00	0.28
CO_3^{2-}						
C	1.68	2.87	12.6	2.3	0.02	28.03
O	1.71	7.44	16.9	2.3	0.01	83.35
H_2CO_3						
C	1.66	3.30	12.7	2.2	0.01	30.06
O _C	1.59	7.10	17.7	2.5	0.02	80.52
O _H	1.61	7.01	17.5	2.5	0.02	80.40
H	0.55	...	2.9	...	0.00	0.27

^a $I = (4\pi\epsilon_0)^{-1} \int \int \rho_a^0(\mathbf{r}_1) \rho_a^0(\mathbf{r}_2) / r_{12} d\mathbf{r}_1 d\mathbf{r}_2$.

remarkably consistent exponent but a variable number of electrons c_2' , depending on the chemical environment. This points to the possibility of transferability of ISA densities between similar atoms.

V. CONCLUSIONS

In conclusion, the ISA method has been introduced as a simple way to partition molecular electron densities into atomic components. The method requires no auxiliary gas-phase calculations for the free atoms and can easily be incorporated into any quantum chemistry software with a DFT integration package. The time required to perform the iterative procedure is typically less than that required to set up the DFT grid, and the procedure scales quadratically with the number of atoms.

ACKNOWLEDGMENTS

The authors thank the Engineering and Physical Sciences Research Council for funding.

¹R. S. Mulliken, *J. Chem. Phys.* **23**, 1833 (1955).

²R. Bader, *Atoms in Molecules* (Oxford University Press, Oxford, 1992).

³F. L. Hirshfeld, *Theor. Chim. Acta.* **44**, 129 (1977).

⁴P. Bultinck, C. V. Alsenoy, P. W. Ayers, and R. Carbó-Dorca, *J. Chem. Phys.* **126**, 144111 (2007).

⁵T. C. Lillestolen and R. J. Wheatley, *Chem. Commun. (Cambridge)* **45**, 5909 (2008).

⁶P. Bultinck, D. L. Cooper, and D. V. Neck, *Phys. Chem. Chem. Phys.* **11**, 3424 (2009).

⁷A. D. Becke, *J. Chem. Phys.* **88**, 2547 (1988).

⁸M. E. Mura and P. J. Knowles, *J. Chem. Phys.* **104**, 9848 (1996).

⁹V. I. Lebedev and D. N. Laikov, *Dokl. Math.* **59**, 477 (1999).

¹⁰O. Treutler and R. Ahlrichs, *J. Chem. Phys.* **102**, 346 (1995).

¹¹P. Stephens, F. Devlin, C. Chabalowski, and M. Frisch, *J. Chem. Phys.* **98**, 11623 (1994).

¹²Basis sets were obtained from the Extensible Computational Chemistry Environment Basis Set Database, Version 02/02/06, as developed and distributed by the Molecular Science Computing Facility, Environmental and Molecular Sciences Laboratory, which is part of the Pacific Northwest Laboratory, P.O. Box 999, Richland, Washington 99352, USA, and funded by the U.S. Department of Energy. The Pacific Northwest Laboratory is a multiprogram laboratory operated by Battelle Memorial Institute for the U.S. Department of Energy under contract DE-AC06-76RLO 1830. Contact Karen Schuchardt for further information.

¹³MOLPRO, a package of *ab initio* programs, H.-J. Werner, P. J. Knowles, R. Lindh, M. Schütz, *et al.*, version 2006.1, (2006) (see: <http://www.molpro.net>).

¹⁴E. M. Mas and K. Szalewicz, *J. Chem. Phys.* **104**, 7606 (1996).

¹⁵J. G. C. M. van Duijneveldt-van de Rijdt, W. T. M. Mooij, and F. B. van Duijneveldt, *Phys. Chem. Chem. Phys.* **5**, 1169 (2003).

¹⁶B. J. Smith, D. J. Swanton, J. A. Pople, H. F. Schaefer III, and L. Radom, *J. Chem. Phys.* **92**, 1240 (1990).

¹⁷A. Jagielska, R. Moszyński, and L. Piela, *J. Chem. Phys.* **110**, 947 (1999).

¹⁸P. M. W. Gill, B. G. Johnson, J. A. Pople, and S. W. Taylor, *J. Chem. Phys.* **96**, 7178 (1992).